

SHIELDING DESIGN IN NEUTRON ACTIVATION EXPERIMENT SYSTEM BASED ON D-T NEUTRON TUBE

by

**Jingfei CAI¹, Shiwei JING^{1,2*}, Dedong HE¹, Yangwenting OU¹,
Xinyi LING¹, and Bingbing LI¹**

¹School of Physics, Northeast Normal University, Jilin, Changchun, China

²China Institute of Atomic Energy, Beijing, China

Scientific paper

<https://doi.org/10.2298/NTRP2201042C>

The deuterium-tritium neutron generator should be fully shielded for the safety of the operators participating in the experiments since the D-T neutron generator is commonly used in activation experiments. In this study, MCNP5 code was used to simulate the shielding effect of the neutron thermalization device previously designed by our group with Pb and boron-containing polyethylene as the shielding material. The neutron dose rate outside of the previous thermalization device can not meet the requirement, so a concrete wall is needed between the device and the operators. Two models are designed with concrete walls. One model is that the device and the experimental operators are not in the same room, another one is that the device and the experimental operators are in the same room, and there is an L-shaped concrete wall between them. In both models, the dose rate to the operators was less than 5 Sv⁻¹.

Key words: MCNP simulation, shielding, D-T modulated neutron initiator, MCNP5 code

INTRODUCTION

Neutron activation analysis is a technique for qualitative and quantitative analysis of elements in substances. It has the advantages of low pollution, simultaneous analysis of multiple elements, high accuracy, non-destructiveness, and high sensitivity. It is widely used in biophysics [1] and environmental monitoring [2, 3], radiography [4, 5], industry [6-8], explosives detection [9-12], and other fields. Learning and mastering the neutron activation analysis technology is very useful for college students. Many colleges commonly use a D-T neutron generator as a neutron source for neutron activation analysis. Since the D-T neutron generator emits neutrons and gamma-rays which will cause radiation damage to personnel, even under the package of the thermalization device, the radiation dose is still far higher than the safe dose value (5 Sv⁻¹) [13]. Therefore, it is necessary to study the entire shielding device. Boron-containing polyethylene (BPE) is a new type of neutron shielding material, which is not only significantly better than polyethylene in shielding thermal neutrons, fast neutrons and, gamma radiation but also has good stability, corrosion resistance, electrical insulation, wear resistance, and other advantages [14-16]. Because lead metal has a

high density, lead is often used as a gamma shield [17]. Therefore, lead and BPE are, respectively, selected as the gamma-ray and neutron shielding materials. To obtain a shielding device suitable for operators to conduct neutron activation analysis experiments, MCNP5 was used to simulate the shielding of the thermalization device, and the results may lay the foundation for future neutron activation experiments.

INITIAL THERMALIZATION DEVICE AND OPTIMIZATION

Initial thermalization device

In this study, NG-9 D-T neutron generator developed by Northeast Normal University was used as the neutron source which can generate 14 MeV neutrons. It consists of a neutron emitter, a corresponding electronic system, and a control box fig. 1(c). The entire neutron emitter is a stainless-steel cylinder with a radius of 4.3 cm and a length of 89 cm fig. 1(a). The Penning ion source, accelerating electrode, reservoir and target are enclosed in a neutron tube. The neutron tube is a cylinder with a radius of 2.5 cm and a length of 10 cm, fig. 1(b). Between the transmitter head and the neutron, the tube is filled with a thickness of 1.7 cm polyimide ($\rho = 1.4 \text{ gcm}^{-3}$), and sulfur hexafluoride

* Corresponding author, e-mail: jingsw504@nenu.edu.cn

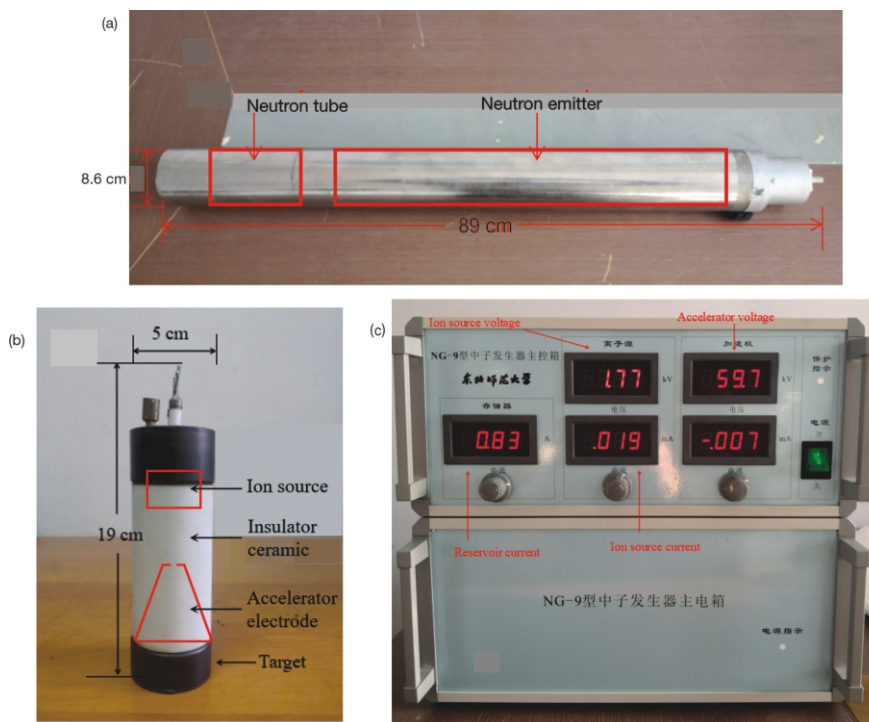


Figure 1. The picture of the NG-9 neutron generator; (a) the emitter of the neutron generator, (b) the neutron tube, and (c) the main control box

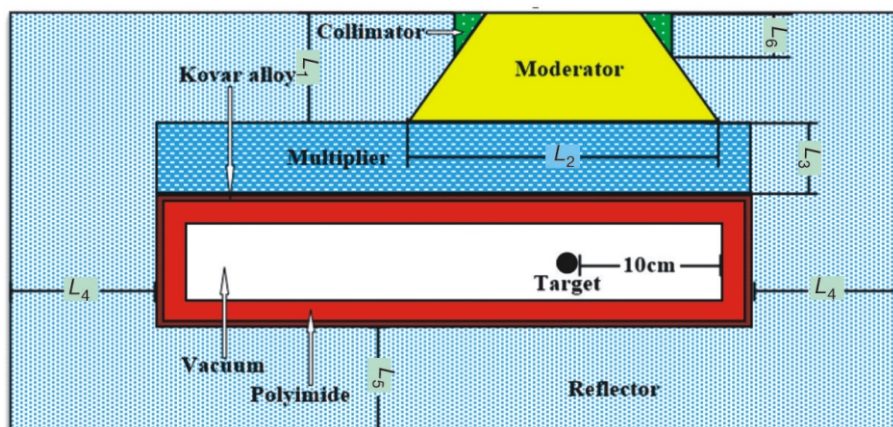


Figure 2. The design of our previous thermalization device

(SF₆) gas is also filled inside the transmitter head. Polyimide and SF₆ gas are used to isolate the high pressure in the neutron emitter from the external environment. The thermalization system designed for NG-9 D-T neutron generator by our group was used as the initial thermalization device [18], which is shown in fig. 2. The specifications of the thermalization device in fig. 2 are as follows: $L_1 = 8$ cm, $L_2 = 20$ cm, $L_3 = 4$ cm, $L_4 = 20$ cm, $L_5 = 25$ cm, and $L_6 = 3.5$ cm. Among them, high-density polyethylene (HDPE) with a density of 0.950 gcm⁻³ is selected as the moderator, lead ($\rho = 11.34$ gcm⁻³) as the multiplier and reflector, and nickel ($\rho = 8.90$ gcm⁻³) as the collimator.

Optimization of initial thermalization device

Let P be the thermal efficiency, eq. (1), which represents the ability of the device to thermalize fast

neutrons. Among them, ϕ_{Th} and ϕ_T , respectively, represent the thermal neutron flux and total neutron flux on the optimized device output surface

$$P = \frac{\phi_{Th}^2}{\phi_T} \quad (1)$$

In this research, the collimator is needed to improve to optimize the thermal device. Change the aperture size of the collimator and use the F2 counter card to measure the thermal neutron flux and total neutron flux on the output surface, to get P . Figure 3 shows the change of P with the aperture of the collimator. It can be seen from fig. 3 that as the aperture size increases, P first increases and then decreases. When the collimating aperture size is 3 cm P reaches its maximum value. So, 3 cm diameter aperture size of the collimator was selected in the subsequent thermalization device.

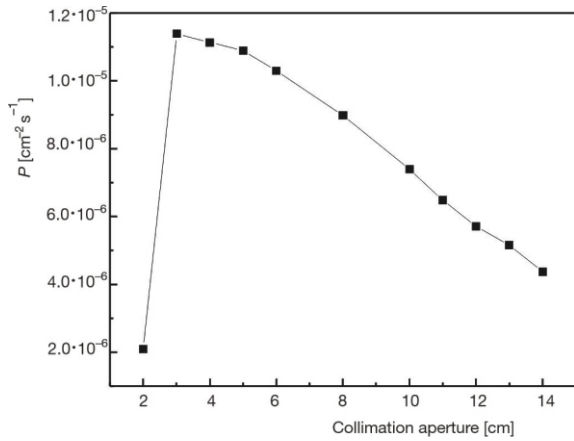


Figure 3. *P* changes with collimation aperture

SHIELDING DESIGN WITHOUT CONCRETE WALL

The first model is without a concrete wall between the device and operators in the room. Operators can directly perform activation experiments in the laboratory after the thermalization device is surrounded by shielding material. The shielding design is shown in fig. 4. The Y-axis and Z-axis are, respectively, along with the axial and radial directions of the emitter of the NG-9 neutron generator. In the Z-axis direction of the shielding device, for the activation experiment, there is a cylindrical cavity (3 cm diameter) filled with air with a height of 15 cm. The air layer is placed on the collimator, which is included in the thermalization device. A layer of 5 % BPE ($\rho = 0.955 \text{ gcm}^{-3}$) with a cylindrical density is first covered based on the thermalization device. Suppose the initial BPE has a radius of 50 cm, a length of 159 cm, and a of 53.5 cm distance from the source on the side close to the source. A layer of cylindrical lead ($\rho = 11.34 \text{ gcm}^{-3}$) is coated on the BPE. The thickness of the lead layer is 5 cm, the length is 169 cm, and the distance from the source close to the source is 58.5 cm, respectively. The bottom surface of the BPE and lead is perpendicular to the XY plane and extends in the Y-axis direction, which is the same as the thermalization device. Then six ballpoints with a radius of 1 cm are set on the surface of the shielding device.

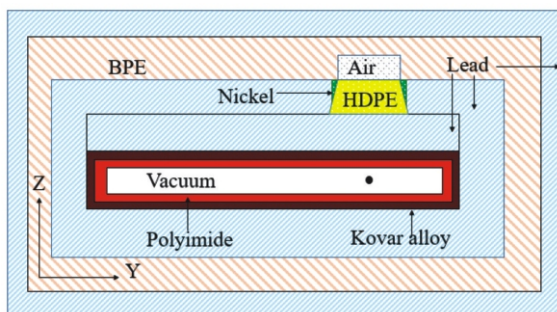


Figure 4. Initial shielding design

Table 1. The initial simulated dose rate (neutron yield is $4 \cdot 10^8 \text{ ns}^{-1}$)

Location	Neutron dose rate [Sv ^h ⁻¹]	Photon dose rate [Sv ^h ⁻¹]	Total dose rate [Sv ^h ⁻¹]
+X	1506.7	19.9	1526.6
-X	1342.0	19.2	1361.2
+Y	1209.7	11.9	1221.6
-Y	50.8	0.4	51.2
+Z	2143.9	19.5	2163.4
-Z	1045.6	14.3	1059.9

These six points are respectively in the X-axis, Y-axis, and Z-axis directions of the emission source. Their flux value is calculated with F5 counter, and the DE and DF counter cards are used to convert the flux in the calculated cell into the environmental dose equivalent $H^*(10)$ [19]. The flux-dose conversion coefficient of neutrons and photons comes from ICRP publication 74 [20]. In this simulation, the number of particles participating in the experiment is $1 \cdot 10^7$, and the output result $H^*(10)$ is all multiplied by $4 \cdot 10^8$ neutrons per second (the maximum yield of the neutron generator) to obtain the neutron, photon dose rate, and total dose rate of the initial shielding design, which are shown in tab. 1.

It shows in tab. 1 that the neutron dose rate and total dose rate are far higher than $5 \text{ Sv}^{\text{h}^{-1}}$ when the BPE radius is 50 cm and the length is 159 cm. When the radius of BPE gradually is increased from 50 cm to 100 cm in steps of 5 cm, at the same time, the thickness of lead is fixed at 5 cm, the variation of the dose rate of each location with the BPE is shown in figs. 5-7.

It can be seen from three figures that the dose rate in the +Y axis and -Y axis only fluctuates slightly without decreasing since only the radius of the BPE is changed. The dose rate of the four directions of the X-axis and Z-axis decreases rapidly with the increase in BPE radius, but the total dose rate everywhere is still higher than $5 \text{ Sv}^{\text{h}^{-1}}$ when the BPE radius is 100 cm. The dose rate in the +Z direction is much larger than that in the other three directions because this direction

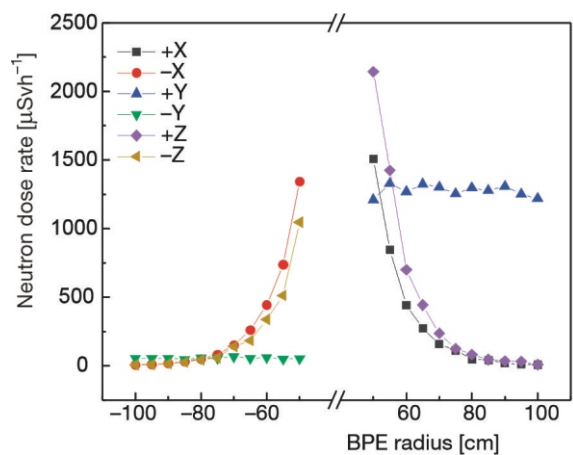


Figure 5. The neutron dose rate changes with BPE radius

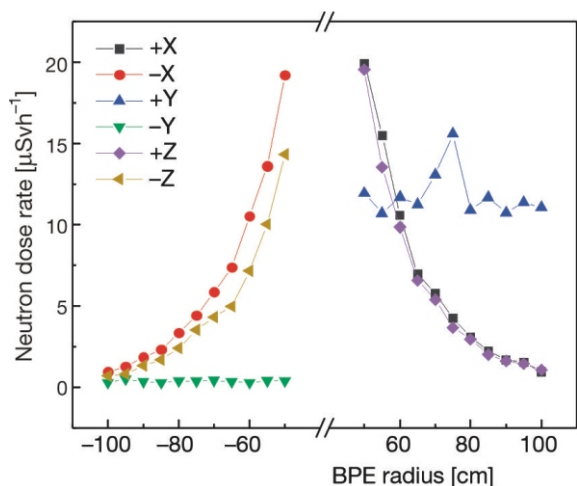


Figure 6. The photon dose rate changes with BPE radius

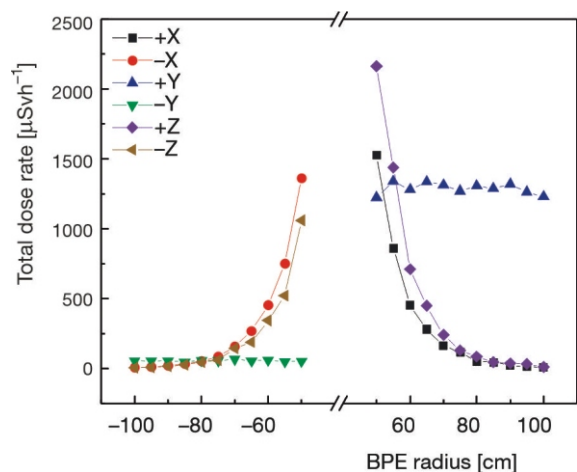


Figure 7. The total dose rate changes with BPE radius

is the output direction of thermal neutrons and there is an air cavity as the neutron activation experiment area.

Boron carbide (B_4C) has the advantages of good neutron shielding performance, low price, easy manufacturing, good high-temperature stability, etc. [21, 22]. A layer of B_4C cylindrical with a radius of 4 cm and a height of 71.9 cm is added above the air cavity. Figure 8 shows the improved device model with B_4C , and the simulation results of six ballpoints on the surface of the shielding device are shown in tab. 2.

It can be seen from tab. 2 that when the radius of the BPE is 100 cm and the length is 159 cm, the neutron dose rate and total dose rate are both higher than 5 Sv h^{-1} at five positions except the $-Z$ axis direction. The dose rate in the two directions of the X -axis is slightly larger than that when there is no B_4C because B_4C has a weak ability to absorb thermal neutrons and BPE has better thermal neutron absorption capacity. Therefore, part of the BPE replaced with B_4C will increase the dose rate in other directions.

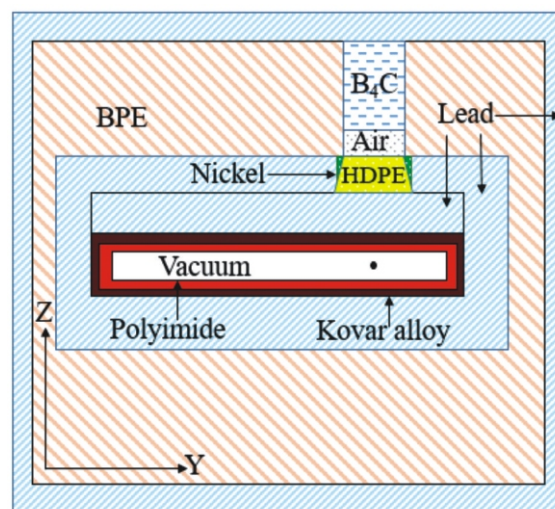


Figure 8. Improved shielding device with B_4C

Table 2. Dose rate after adding B_4C and when BPE radius is 100 cm (neutron yield is $4 \cdot 10^8 \text{ ns}^{-1}$)

Location	Neutron dose rate [Sv h ⁻¹]	Photon dose rate [Sv h ⁻¹]	Total dose rate [Sv h ⁻¹]
+X	8.5	1.1	9.6
-X	5.7	1.1	6.8
+Y	1202.7	11.5	1214.2
-Y	52.3	0.3	52.6
+Z	5.0	0.4	5.4
-Z	3.1	0.8	3.9

THE SHIELDING DESIGN WITH WALL

Considering the cost and the safety of operators, a concrete wall is added as a gap between the operators and the experimental instrument. There are two cases to be considered to change the wall-less shielding to wall shielding.

The operator and the instrument are not in the same laboratory

In this case, the device is placed in the laboratory and the operators conduct experiments in the control room outside the laboratory, which means the operators are in different rooms with the device. The selected laboratory is 577 cm long, 349 cm wide and 315 cm high respectively, along the Z -axis, Y -axis, and X -axis directions. The thickness of concrete wall of the laboratory room is 26 cm. The device is placed in the center of the YZ plane of the room, 15 cm away from the ground ($+X$ axis direction). The device model is shown in fig. 9. Set six ballpoints with a radius of 1cm on the outer wall of the laboratory. Six points are respectively in the positive and negative directions of the emission source along the X -axis, Y -axis, and Z -axis of the lab room. The neutron dose rate, photon dose rate,

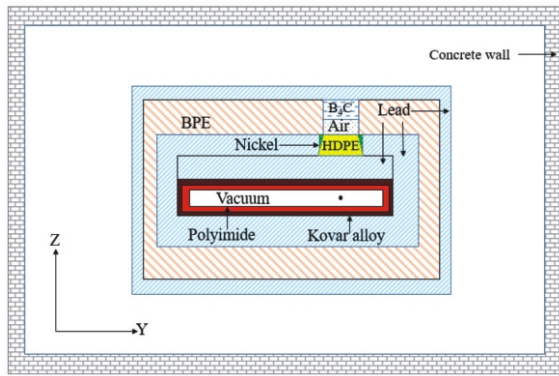


Figure 9. Outdoor shielding design (not in scale)

Table 3. Outdoor shielding dose rate when the BPE radius is 50 cm (neutron yield is $4 \times 10^8 \text{ s}^{-1}$)

Location	Neutron dose rate [Sv h^{-1}]	Photon dose rate [Sv h^{-1}]	Total dose rate [Sv h^{-1}]
+X	46.5	3.2	49.7
-X	4.7	0.5	5.2
+Y	13.6	0.5	14.1
-Y	2.1	0.2	2.3
+Z	4.1	0.4	4.5
-Z	3.8	0.3	4.1

Table 4. The total dose rate of different materials [Sv h^{-1}] (neutron yield is $4 \times 10^8 \text{ s}^{-1}$)

Location	BPE	Concrete	HDPE	H ₂ O	D ₂ O
+X	19.7	17.2	15.1	15.8	13.8
-X	5.1	10.4	6.1	4.5	4.7
+Y	5.0	4.3	5.0	4.4	3.9
-Y	12.6	1.9	10.4	9.0	3.3
+Z	5.6	4.3	4.1	3.0	4.3
-Z	2.3	3.0	2.6	3.3	3.1

and total dose rate of these six points are simulated when the BPE radius is 50 cm, the length 150 cm, and the radius of lead is 55 cm and 160 cm in length, which are shown in tab. 3.

It can be seen from tab. 3 that when the BPE radius is 50 cm, the total dose rate in -Y, +Z, and -Z direction is less than 5 Sv h^{-1} , which meets the safety dose requirement. The dose rate in the +Y is much higher than that in -Y direction because the detection point in the +Y is close to the position of the emission source. It is needed to increase the thickness of the BPE in +Y and reduce the thickness of the BPE in -Y direction. The thickness of the BPE in the +Y direction is increased by 3 cm, and the thickness of the BPE in the -Y direction is reduced to zero. A 15 cm thick shielding plank can be placed in this direction and the device can be placed on this plank because the dose rate in +X direction is far higher than the safe value. The materials selected for the shielding board are concrete, water (H₂O), HDPE, BPE, and heavy water (D₂O). The dose rate of six points under different shielding materials is shown in tab. 4.

It can be seen from tab. 4 that regardless of the material, the dose rate in the +X direction is higher than 5 Sv h^{-1} , and the dose rate in the -Y direction is mostly higher than 5 Sv h^{-1} . A double-layer material is considered to use as a shielding plate. It can be seen from tab. 4 that under the condition of using HDPE, H₂O, and D₂O as shielding plates, the dose rate in the +X direction is lower. Considering the cost, HDPE and H₂O are chosen as the double-layer material, at the same time, to raise the device 10 cm, that is, 25 cm from the ground. The dose rate in the -Y direction is higher under the condition of HDPE and H₂O, so a layer of 110 cm \times 10 cm \times 110 cm water wall can be placed in the -Y direction. For the shielding plate, considering that the cost of the water wall is lower than that of HDPE, first fix the HDPE thickness to 10 cm and change the thickness of the water wall. The total dose rate change at each measurement point is shown in fig. 10. It can be seen from the figure that as the thickness of the water wall increases, the dose rate in the +X direction decreases, but it is still higher than 5 Sv h^{-1} , and the dose rate in other directions has increased at some stage as the thickness of the water wall increases. This may be due to the effect of the water wall on the neutrons' reflection effect. From the figure, the overall shielding effect is better when the thickness of the water wall is 5 cm. So, keep the thickness of the water wall at 5 cm, the HDPE thickness increased from 10 cm to 20 cm in steps of 5 cm, and the thickness of HDPE is 25 cm, the thickness of the water wall is 0 cm. The total dose rate at each point varies with the thickness of HDPE as shown in. It can be seen, fig. 11, that the shielding effect is the best when the thickness of HDPE is 20 cm, but the dose rate in the -X direction is slightly higher than 5 Sv h^{-1} . A water wall with a size of 5 cm \times 93.7 cm \times 110 cm is needed to install on the wall in this direction to reduce the dose rate, as well as to ensure the safety of the operators in this direction. The dose rate after adding the water wall, tab. 5, shows that the dose rate at each point is less than 5 Sv h^{-1} af-

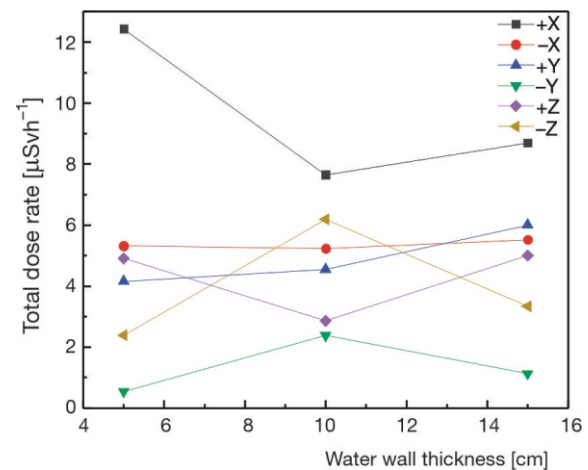


Figure 10. The total dose rate at the measurement point with the thickness of the water wall

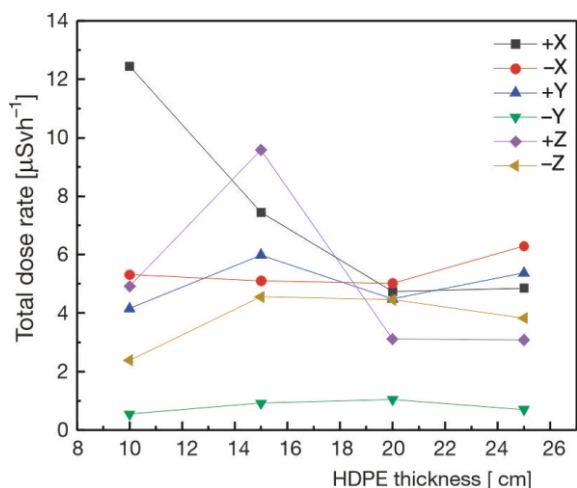


Figure 11. The total dose rate at the changes measurement point changes with the HDPE thickness

Table 5. Dose rate at each point after adding water wall in X direction (neutron yield is $4 \cdot 10^8 \text{ s}^{-1}$)

Location	Neutron dose rate [Sv h ⁻¹]	Photon dose rate [Sv h ⁻¹]	Total dose rate [Sv h ⁻¹]
+X	4.1	0.7	4.9
-X	2.6	0.4	3.0
+Y	3.7	0.4	4.1
-Y	1.0	0.1	1.1
+Z	2.7	0.3	3.0
-Z	2.9	0.4	3.3

ter adding the water wall in the -X direction, which reaches the safe dose rate standard.

The operator and the instrument are in the same laboratory

In this case, a concrete wall will be placed in the laboratory, so that the operator and the device can be in a room. This case is considered for the condition of lack of laboratories. The selected laboratory model is the same as the previously mentioned mode. For this model, the BPE radius is 50 cm and the length is 150 cm, the lead radius is 55 cm and the length is 160 cm. An L-shaped concrete wall is designed to surround the device, and six detection points Y1, Y2, Y3, Z1, Z2, and Z3 along the wall are set, fig. 12. The initial thickness of the L-shaped concrete wall is supposed to be 20 cm, with 5 cm as a step length the dose rate at six points under different concrete thicknesses is shown in figs. 13-15.

It can be seen from the figures that when the thickness of the concrete wall is 50 cm, the dose rate of Z3 and Y2 is still higher than 5 Sv h^{-1} . Double-layer materials such as the shielding wall are designed, considering that the size of the space in the laboratory is not suitable for such a thick concrete wall, as well as

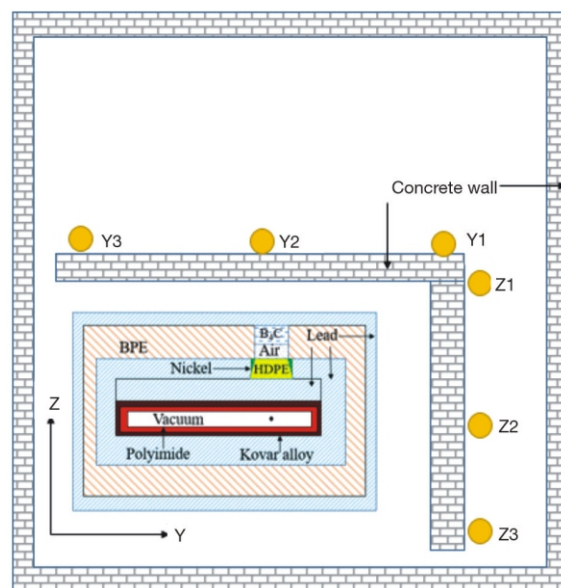


Figure 12. L-shaped concrete wall

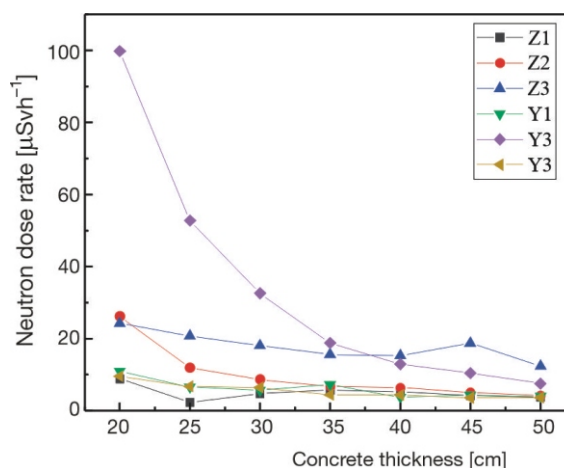


Figure 13. The neutron dose rate changes with concrete thickness

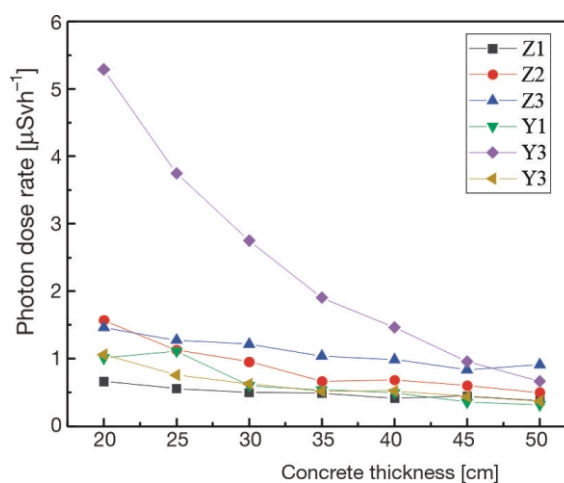


Figure 14. The photon dose rate changes with concrete thickness

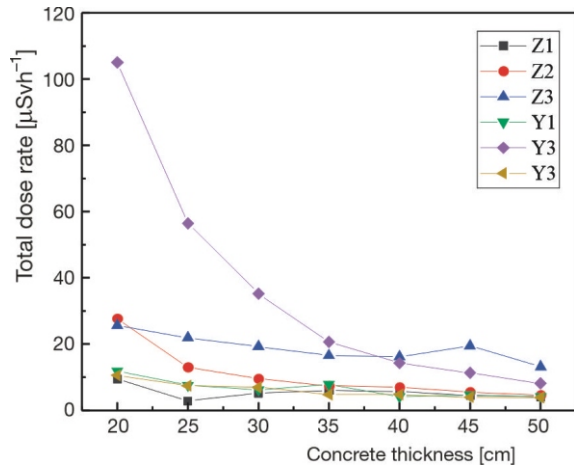


Figure 15. The total dose rate changes with concrete thickness

the cost and difficulty of production. It can be seen from figs. 13-15 that when the thickness of the concrete wall reaches 35 cm, the rate of dose rate changes little with the increase of wall thickness, so select a 35 cm thick concrete wall. Then a layer of shielding material with a thickness of 10 cm is added to the wall near the side of the device. Water, HDPE, BPE, and heavy water are selected as shielding materials. The total dose rate at six points after adding different shielding layers is shown in tab. 6.

It can be seen from the table that HDPE and D₂O have good shielding effects, but the total dose rate at multiple locations is higher than 5 Sv⁻¹. Another layer of material for shielding should be added, for example, HDPE and D₂O. A layer of 5 cm thick D₂O is added on the side of the original HDPE near the device, and the total dose rate after adding a layer of 5 cm thick HDPE on the side of the original D₂O near the device is calculated and shown in tab. 7. It can be seen from tab. 7 that the overall shielding effect of the latter model is better than that of the former one, but the total dose rate of Z3 and Y2 is still higher than 5 Sv⁻¹. Under this condition, the device is changed to the -Z direction, there is a 20 cm air layer between the shielding layer and the device in the Z direction. After moving, the total dose rate results are shown in tab. 7. The total dose rate at Z2 is higher than 5 Sv⁻¹. In order to reduce the dose rate at this point, a layer of 5 cm thick water wall is added outside the concrete wall with the

Table 6. The total dose rate of measurement points under different materials (Sv⁻¹) (neutron yield is 4 10⁸ s⁻¹)

Location	Air	BPE	HDPE	H ₂ O	D ₂ O
Z1	6.1	4.3	4.2	4.1	3.5
Z2	7.4	6.0	5.1	5.2	3.9
Z3	16.5	18.5	16.8	13.9	10.3
Y1	7.8	3.2	3.7	3.12	5.0
Y2	20.6	12.3	11.3	12.1	10.3
Y3	4.8	3.5	4.5	3.3	3.5

Table 7. The total dose rate of each point under double shielding and after adding the air layer (Sv⁻¹) (neutron yield is 4 10⁸ s⁻¹)

Location	10 cm HDPE + 5 cm D ₂ O	10 cm D ₂ O + 5 cm HDPE	Adding air layer
Z1	3.7	3.9	4.3
Z2	5.0	4.6	6.2
Z3	13.5	14.3	14.2
Y1	3.0	3.1	3.4
Y2	9.1	8.5	7.2
Y3	4.7	3.0	3.2

Z-axis in the radial direction. Since the dose rate of Z3 is close to three times the safe dose rate, it is more dangerous to stay around Z3. Therefore, the scope of activities of teachers and operators during the experiment is adjusted to the outer side of the concrete wall with the axial direction of +Y, and three dose rate measurement points Y4, Y5, Y6 that are on the same line as Y1, Y2, and Y3 are added to confirm the dose rate on this straight line. The configuration of the device is shown in fig. 16 and the dose rate at each point are shown in tab. 8. It can be seen from tab. 9 that the dose

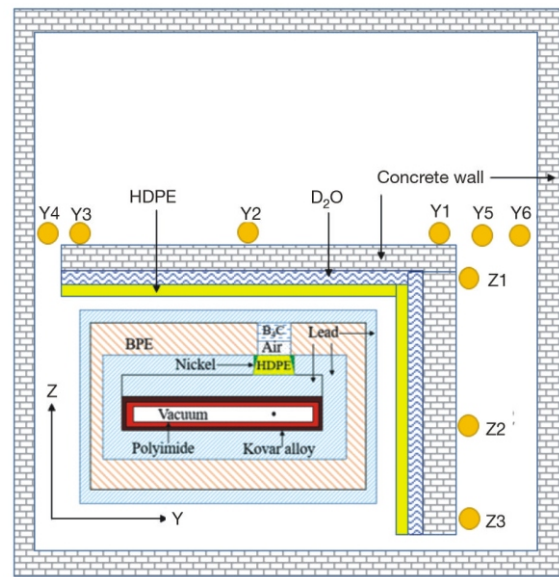


Figure 16. The distribution of Y1 to Y6 (not in scale)

Table 8. Dose rate at each point after adding water layer and after adding two layers of water layer (neutron yield is 4 10⁸ s⁻¹)

Location	Neutron dose rate [Sv ⁻¹]		Photon dose rate [Sv ⁻¹]		Total dose rate [Sv ⁻¹]	
	One water layer	Two layers of water	One water layer	Two layers of water	One water layer	Two layers of water
Y1	2.8	2.1	0.3	0.4	3.1	2.5
Y2	3.7	3.2	0.5	0.2	4.2	3.4
Y3	2.5	2.8	0.3	0.3	2.8	3.1
Y4	4.4	2.4	0.3	0.3	4.7	2.7
Y5	5.2	2.8	0.3	0.4	5.5	3.2
Y6	4.9	2.0	0.3	0.4	5.2	2.4

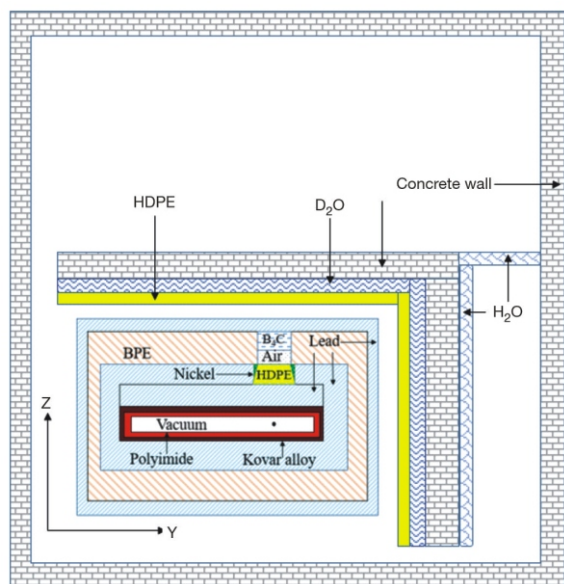


Figure 17. The structure of the final design (not in scale)

rate at Y5 and Y6 is slightly higher than 5 Sv h^{-1} . A layer of 5 cm thick water wall is added along the Y-axis in the radial direction to connect it with the L-shaped concrete wall to form a T-shape. The dose rate of Y1-Y6 (shown in tab. 8) is less than 5 Sv h^{-1} , which is lower than the safe dose value after adding the water wall. The final simulation device is shown in fig. 17.

CONCLUSIONS

In this work, Monte Carlo simulation is used to design a shielding system for the thermalization device based on an NG-9 D-T neutron generator for protecting the safety of the teachers and students participating in the experiment. After calculation for the thermalization device with BPE for neutron shielding and Pb for photon shielding, the results show that the dose rate around the device is higher than the safe dose value even when the volume of the shielding material is relatively larger enough. The models with shielding walls are designed including two cases. One case is that the experimental device and the participants are in the different laboratory rooms. The other is that the experimental device and the operators are in the same lab, but there is an L-shaped concrete wall as a partition. The dose rate is lower than the safe dose value after optimization design, which may be a reference for operators of neutron activation experiments based on the D-T generator.

ACKNOWLEDGMENT

This work was supported by the Department of Science and Technology of Jilin Province of China (20190303101SF).

AUTHORS' CONTRIBUTIONS

J. Cai is the first author of the paper, and she is the main implementer and one of the thought contributors to the research. S. Jing is the corresponding author of the paper, and he is the main thought contributor of the research. The other authors are all supporters of the research.

REFERENCES

- [1] Marchese, N., *et al.*, New Generation Non-Stationary Portable Neutron Generators for Biophysical Applications of Neutron Activation Analysis, *BBA – General Subjects*, 1861 (2017), 1, pp. 3661-3670
- [2] Doron, O., *et al.*, MCNP Benchmarking of an Inelastic Neutron Scattering System for Soil Carbon Analysis, *Nuclear Instruments and Methods in Physics Research A*, 735 (2014), 6, pp. 431-436
- [3] Hei, D. Q., *et al.*, Heavy Metals Detection in Sediments Using PGNAA Method, *Applied Radiation and Isotopes*, 112 (2016), 6, pp. 50-54
- [4] Kwak, J. G., *et al.*, Neutron Emission in Neutral Beam Heated KSTAR Plasmas and its Application to Neutron Radiography, *Fusion Engineering and Design*, 111 (2016), 6, pp. 608-612
- [5] Zhang, J., *et al.*, Design of Collimation Shield for fast Neutron Radiography Based on DT Compact Neutron Source and Simulation of Neutron Beam Characteristics, *Nuclear Physics Review*, 34 (2017), 4, pp. 762-767
- [6] Liu, J., Application of Monte Carlo Simulation Method in the Neutron Coal Quality Analysis Experiment to Study the Change of Coal Seam Thickness, Northeast Normal University, Changchun, 2009
- [7] Reyhancan, I. A., *et al.*, A Monte Carlo Library Least Square approach in the Neutron Inelastic-scattering and Thermal-capture Analysis (NISTA) process in bulk coal samples, *Nuclear Instruments and Methods in Physics Research A*, 843 (2017), 6, pp. 29-33
- [8] A. A. Naqvi, *et al.*, Prompt Gamma-Ray Analysis of Chlorine in Superpozz Cement Concrete, *Nuclear Instruments and Methods in Physics Research A*, 693 (2012), 6, pp. 67-73
- [9] Sharma, S. K., *et al.*, Explosive Detection System Using Pulsed 14 MeV Neutron Source, *Fusion Engineering and Design*, 85 (2010), 7, pp. 1562-1564
- [10] Han, M. C., *et al.*, Experiment and MCNP Simulation of a Portable Tagged Neutron Inspection System for Detection of Explosives in a Concrete Wall, *Nuclear Instruments and Methods in Physics Research A*, 929 (2019), pp. 156-161
- [11] Jiang, Z., Research on the Detection of Shallow Buried Explosives in Soil Based on PGNAA Technology, Nanjing University of Aeronautics and Astronautics, Nanjing, 2017
- [12] Ivannikov, S. I., *et al.*, Determination of Uranium in Solutions by the Neutron Activation Analysis Method with ^{252}Cf Radionuclide Neutron Source, *Nucl Technol Radiat*, 36 (2021), 1, pp. 12-17
- [13] ***, ICRP-International Commission on Radiological Protection, Recommendations of the International Commission on Radiological Protection, ICRP Publication 60, Ann. ICRP 21, (1990), 1-3
- [14] Pang, M., *et al.*, MC Simulation Study of D-T Neutron Source Shielding in Coal Quality Detection System, *Physics Experiment*, 38 (2018), 7, pp. 8-13

- [15] Zhang, Q. W., et al., Research on the Neutron Shield and Absorber of Gamma Total Absorption BaF₂ Detector[J], *Nuclear Physics Review*, 37 (2020), 3, pp. 771-776
- [16] Liu, Y. X., et al., Monte Carlo Simulation Study on the ²⁴¹Am-Be Radionuclide Source Reference Neutron Radiation, *Nucl Technol Radiat*, 35 (2020), 4, pp. 283-293
- [17] Zhang, Q. W., et al., Research on the Neutron Shield and Absorber of Gamma Total Absorption BaF₂ Detector, *Nuclear Physics Review*, 37 (2020), 03, pp. 771-776
- [18] Li, C., Monte Carlo Simulation Study on Slowing Down and Shielding System of D-T Neutron Generator, Northeast Normal University, Changchun, 2020
- [19] Hernandez-Adame, P. L., et al., Design of an Explosive Detection System Using Monte Carlo Method, *Applied Radiation and Isotopes*, 117 (2016), 11, pp. 27-31
- [20] ***, ICRP-International Commission on Radiological Protection, Conversion Coefficients for Use in Radiological Protection Against External Radiation, ICRP Publication 74, *Ann. ICRP* 26 (1996), 3-4, pp. 47-54
- [21] Gong, J. J., et al., Design, Preparation and Performance Study of a New High-Temperature Resistant Neutron Shielding Composite Material, *Atomic Energy Science and Technology*, 55 (2021), 7, pp. 1323-1330
- [22] Shi, Y., et al., Research on the Shielding and Mechanical Properties of High-Density Polyethylene/Lead-Boron Composites, *China Plastics*, 34 (2020), 1, pp. 51-57

Received on January 23, 2022

Accepted on May 24, 2022

Бингфеј ЦАЈ, Шивеј ЂИНГ, Дидунг ХЕ, Јангвентинг ОУ, Синји ЛИНГ, Бингбинг ЛИ

ДИЗАЈН ЗАШТИТЕ СИСТЕМА ЕКСПЕРИМЕНТА ЗА АКТИВАЦИЈУ НЕУТРОНА ЗАСНОВАНОГ НА ДЕУТЕРИЈУМ-ТРИЦИЈУМСКОЈ НЕУТРОНСКОЈ ЦЕВИ

Деутеријум-трицијумски генератор неутрона треба да буде потпуно заштићен ради безбедности оператора који учествују у експериментима јер се деутеријум-трицијумски генератор неутрона обично користи у експериментима активације. У овој студији, МЦНП5 код коришћен је за симулирање ефекта заштите уређаја за термализацију неутрона који је претходно дизајниран са оловом и полиетиленом који садржи бор као заштитни материјал. Јачина дозе неутрона у околини претходног уређаја за термализацију не задовољава, тако да је потребан бетонски зид између уређаја и оператора. Два модела пројектована су са бетонским зидом. Један је да уређај и експериментални оператори нису у истој просторији, а други је да су уређај и експериментални оператори у истој просторији а између њих је бетонски зид у облику слова L. У оба модела, јачина дозе за операторе била је мања од $5 \mu\text{Sv h}^{-1}$.

Кључне речи: МЦНП симулација, заштитни, деутеријум-трицијумски модулисани неутронски иницијатор, МЦНП код